Journal of Trace Elements in Medicine and Biology 51 (2019) 19–27

Contents lists available at ScienceDirect

Journal of Trace Elements in Medicine and Biology

journal homepage: www.elsevier.com/locate/jtemb

Low doses of methylmercury exposure during adulthood in rats display oxidative stress, neurodegeneration in the motor cortex and lead to impairment of motor skills

Luana Nazaré da Silva Santana[a], Leonardo Oliveira Bittencourt[a], Priscila Cunha Nascimento[a], Rafael Monteiro Fernandes[a], Francisco Bruno Teixeira[a], Luanna Melo Pereira Fernandes[a], Marcia Cristina Freitas Silva[a], Lygia Sega Nogueira[a], Lílian Lund Amado[c], Maria Elena Crespo-Lopez[d], Cristiane do Socorro Ferraz Maia[b], Rafael Rodrigues Lima[a,*]

[a] Laboratory of Functional and Structural Biology, Institute of Biological Sciences, Federal University of Pará, Belém, PA, Brazil
[b] Laboratory of Pharmacology of Inflammation and Behavior, Institute of Health Sciences, Federal University of Pará, Belém, PA, Brazil
[c] Laboratory of Ecotoxicology, Institute of Biological Sciences, Federal University of Pará, Belém, PA, Brazil
[d] Laboratory of Molecular Pharmacology, Institute of Biological Sciences, Federal University of Pará, Belém, PA, Brazil

ARTICLE INFO

Keywords:
Organomercury compound
Organic mercury
Oxidative stress
Neurodegeneration
Motor function

ABSTRACT

Despite the vast distribution among tissues, the central nervous system (CNS) represents the main target of methylmercury (MeHg) toxicity. However, few studies have evaluated the effects of MeHg exposure on the CNS at equivalent doses to human environmental exposure. In our study, we evaluated the motor cortex, an important area of motor control, in adult rats chronically exposed to MeHg in a concentration equivalent to those found in fish-eating populations exposed to mercury (Hg). The parameters evaluated were total Hg accumulation, oxidative stress, tissue damage, and behavioral assessment in functional actions that involved this cortical region. Our results show in exposed animals a significantly greater level of Hg in the motor cortex; increase of nitrite levels and lipid peroxidation, associated with decreased antioxidant capacity against peroxyl radicals; reduction of neuronal and astrocyte density; and poor coordination and motor learning impairment. Our data showed that chronic exposure at low doses to MeHg is capable of promoting damages to the motor cortex of adult animals, with changes in oxidative biochemistry misbalance, neurodegeneration, and motor function impairment.

1. Introduction

One of the most toxic forms of mercury (Hg) for living animals is the organic compound methylmercury (MeHg) [1], which is formed by methylation of Hg^{+2} by methanogenic and sulfate-reducing bacteria in aquatic ecosystems and soils. Human exposure to MeHg occurs primarily *via* diet, specifically through ingestion of contaminated seafood, mainly for long periods and at low doses [2–4].

MeHg at a low dose has the ability to affect the neuronal systems and to hinder the development of behavioral domains, such as various cognitive functions [5]. Chronic exposure using a low dose of MeHg mimics the lifelong exposure and may not induce visible symptoms [6]. However, Kong et al. [7] demonstrated a general state of metabolic deficit in the somatosensory cortex, besides decreased levels of pyruvate, ATP, and total calcium ions in rats exposed to 40 μg MeHg/kg body weight/day. The latter dose is equivalent to approximately 2 μg/g in human hair, according to a 250:5:1 ratio for hair:brain:blood contents [8], which is usually the minimum level of Hg found in chronically exposed populations, such as those in the Amazon [3,9.

Once inside the human body, MeHg is present as a water-soluble complex if not attached to thiol ligands. Generally, MeHg reacts with sulfhydryl (–SH) or selenohydryl (–SeH), which is a nucleophile of biomolecules like proteins. During interactions, oxidative stress may occur due to depletion of antioxidants and increased formation of reactive oxygen species (ROS). ROS may lead to damage of enzymes, nucleic acid, and lipids, which may proceed to cell death [10]. Despite the vast distribution among tissues, the central nervous system (CNS) represents the main target of toxicity [11].

* Corresponding author at: Laboratory of Functional and Structural Biology, Institute of Biological Sciences, Federal University of Pará, Street Augusto Corrêa N. 1, Campus do Guamá, Belém, PA, 66075-900, Brazil.
E-mail address: rafalima@ufpa.br (R.R. Lima).

https://doi.org/10.1016/j.jtemb.2018.09.004
Received 3 July 2018; Received in revised form 21 August 2018; Accepted 10 September 2018

Thus, our study aimed to investigate the effects of chronic and low-dose exposure to MeHg (40 µg/kg/day for 60 days) in adult rats and its reflection in the motor cortex, an important area of motor control functions, under oxidative biochemistry and tissue perspectives, which could be associated to motor skill impairment.

2. Material and methods

2.1. Animals and experimental design

Forty Male Wistar rats, weighing 150–200 g and 90 days old, were used in this investigation under the protocol CEPAE-UFPA: 225-14, following the NIH Guide for the Care and Use of Laboratory Animals. Animals were maintained in collective cages (four animals each) and kept in a climate-controlled room (25 °C) with a 12:12 h light/dark cycle (lights on at 7:00 A.M.) and water and food *ad libitum*.

Animals were divided into two groups. The first group (n = 20) received MeHg (40 µg/kg/day) diluted in corn oil by oral gavage for 60 days, while the second group (n = 20) received the equivalent volume administered to the exposed group, by oral gavage, containing only the vehicle of dilution for the same time. The MeHg dose was adjusted weekly after weighting of the animals. In recent works from our group, we validated this model of exposure to MeHg (administered by gavage during 60 days) [12,13] adapted from Kong et al. [7], in which they suggested that this concentration of MeHg is able to promote Hg systemic distribution and triggers biochemical and molecular alterations in brain regions. The experimental design of all methodological steps is summarized in Fig. 1.

2.2. Behavioral assessment

Twenty-four hours after the end of the exposure period, the animals were taken to an assay room 1 h before the behavioral tasks for habituation and then submitted to behavioral tests. For the behavioral tests, 10 animals per group were used.

2.2.1. Open field test

To evaluate spontaneous locomotion, exploratory activity was assessed by the number of quadrants crossed [14]. In order to prevent a possible anxiety component on motor performance that could compromise the results, we analyzed peripheral and central distances. Animals were placed on an arena measuring 100 × 100 x 40 cm, with the floor divided into 25 equal quadrants (20 x 20 cm). Initially, each animal was placed in the center of the floor and observed for 5 min. The number of total intersections and the distances measured were analyzed by Software Any-maze™ V. 4.99 (Stoelting Co., USA).

2.2.2. Rotarod test

To evaluate motor coordination and balance through a forced task, we employed the rotarod test [15] on Insight's apparatus (Insight, Brazil). The protocol used was previously published by Teixeira et al. [16], which consists in training the animals to self-maintain over the rotating rod for 3 min at 16 rotations per minute (rpm). After training, the animals were tested by latency until the first fall with a cut-off 3 min. The analyses were repeated three times with 120-second intervals.

2.3. Total mercury accumulation

After the exposure period, 10 animals per group were euthanized through cervical dislocation, followed by brain removal and motor cortex dissection. One hemisphere was used for measurement of total Hg accumulation (THg), while the other hemisphere was used for oxidative biochemistry analysis.

To determine the THg in motor cortex assay, the samples were treated according to Akagi et al. [17] method and as previously performed by our group [12,13], which consists in wet digestion of samples through homogenizing a wet sample (weighting 0.5 g maximum);

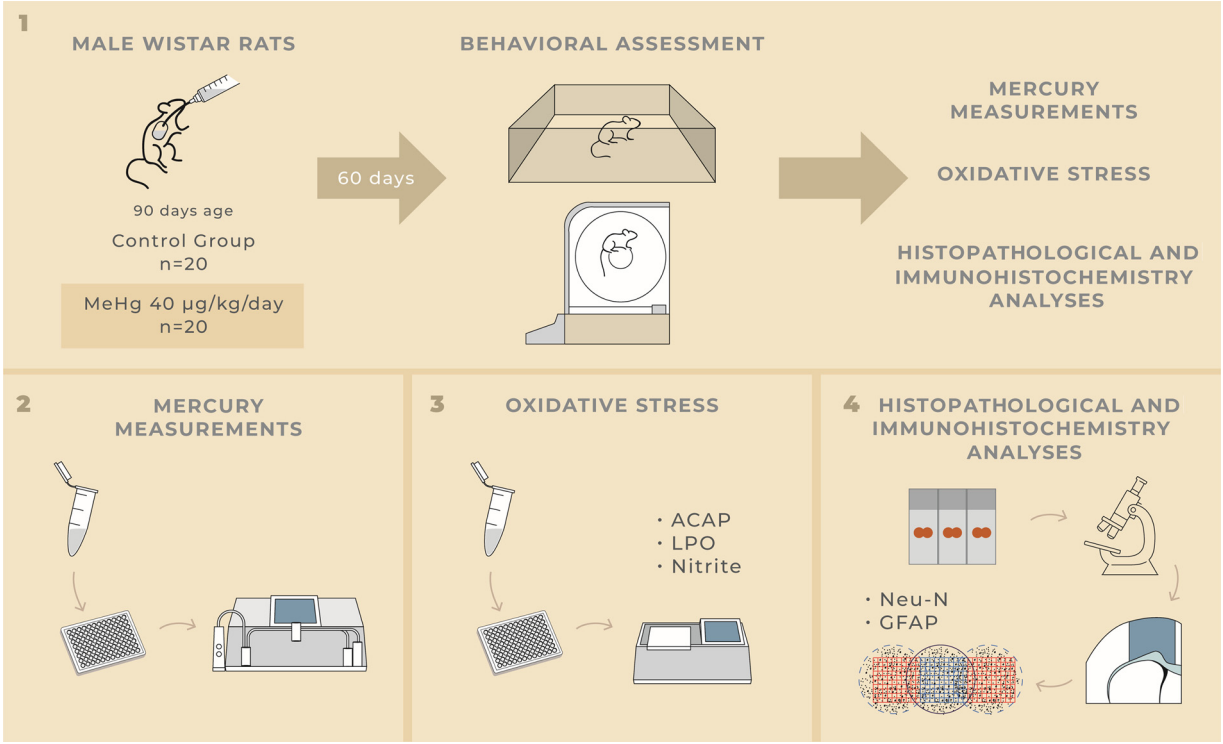

Fig. 1. Experimental steps. Sample description and model of exposure to MeHg; Open Field and Rotarod as motor tests; division of experimental groups and animal destination for each stage of analysis (1); total mercury measurement assay (2); Lipid Peroxidation (LPO), Nitrites Levels (Nitrite) and Antioxidant Capacity Against Peroxyl Radicals (ACAP) as oxidative biochemistry assays (3); immunohistochemistry and quantitative analyses of neurons (Neu-N) and astrocytes (GFAP) (4).

adding 1 mL of distilled water, 2 mL of nitric acid-perchloric acid 1:1 (v:v) (HNO_3-$HClO_4$), and 5 mL of sulfuric acid (H_2SO_4); and maintaining on a heat plate (200–230 °C) for 30 min. THg measurements were performed through atomic absorption spectrometry (Semi-automated Mercury Analyzer, Model Hg-201, Sanso Seisakusho Co., Ltd., Tokyo, Japan), expressing results in μg/g.

2.4. Biochemical analyses

In the biochemical analyses, all samples were individually stored in microtubes and immediately frozen in liquid nitrogen until execution of the homogenization with Tris-HCl buffer (pH: 7.4). Aliquots from this homogenate were separated individually and used for the analyses described below.

2.4.1. Antioxidant capacity against peroxyl radicals

Total antioxidant capacity against peroxyl radicals was analyzed through ROS determination in samples with fixed protein concentration (2.5 μg/μL) incubated or not with a peroxyl radical generator. The detailed methodology is described by Amado et al. [18]. Peroxyl radicals were produced by thermal (35 °C) decomposition of 2,2´-azobis 2 methylpropionamidine dihydrochloride (ABAP; 4 mM; Aldrich). For ROS determination, we employed the fluorogenic compound 2´,7´-dichlorofluorescin diacetate (H2DCF-DA) at a final concentration of 40 mM. H2DCF-DA passively diffuses through cellular membranes and once inside the acetates is cleaved by intracellular esterases. Thereafter, the non-fluorescent compound H2DCF is oxidized by ROS to the fluorescent compound DCF. The readings were made in a fluorescence microplate reader (Victor 2, Perkin Elmer) every 5 min for 1 h. Background fluorescence was determined before the addition of DCF-DA. Total fluorescence production was calculated by integrating the fluorescence units (FU; y axis) along the time of the measurement (x axis), after adjusting FU data to a second-order polynomial function. The results were calculated as the area difference of FU x min in the same sample with and without ABAP addition and standardized to the ROS area without ABAP (background area). Using this methodology, a reduced relative area means higher antioxidant capacity, because low fluorescence levels obtained after the addition of ABAP indicate high competence in neutralizing peroxyl radicals. For a direct reading of the results, the inverse of relative difference between the ROS areas with and without ABAP was considered a measure of antioxidant capacity. The results were expressed as percentage of control.

2.4.2. Nitrite concentration and lipid peroxidation

An aliquot from the homogenate of each sample described above was centrifuged at 21.000 g for 20 min at 4 °C, and the supernatant was used to measure nitrite levels originally according to Green et al. [19] and adapted by our study group through Teixeira et al. [20]. Samples were incubated in a 96-well microplate at room temperature with Griess reagent (0.1% *N*-[1-naphthyl] ethylenediaminedihydrochloride; 1% sulfanilamide in 5% phosphoric acid; 1:1). After 20 min, the absorbance was measured at 550 nm of wavelength and compared to those of standard solutions of sodium nitrite.

In the case of lipid peroxidation (LPO), we measured malondialdehyde (MDA) levels as previously described by Souza-Monteiro et al. [21]. Briefly, after centrifugation of the samples at 2500 g for 10 min, a solution containing methanesulfonic acid and *N*-methylphenyl indole (10.3 mM in acetonitrile) diluted in methanol (1:3) was added to the supernatants and incubated for 40 min at 4 °C. Absorbance was measured at 570 nm and compared to standard concentrations of MDA.

In both assays of prooxidative agents described above, we corrected the levels of nitrites and MDA by quantification of total proteins based on Bradford's [22] method. The results were expressed as percentage of control.

2.5. Histopathological and immunohistochemistry analyses

After behavioral assessment, 10 animals (different from those for biochemical and THg analyses) of each group were used for tissue analyses. The animals were deeply anesthetized (ketamine) and transcardially perfused with heparinized 0.1 M phosphate-buffered saline (PBS) followed by 4% paraformaldehyde. The brains were removed by craniotomy and post-fixed for 4 h in Bouin solution. Then, the specimens were dehydrated in increasing ethanol solutions (70%, 80%, 90%, absolute 1, and absolute 2), diaphanized in xylene, and embedded in paraplast (MCCormick®). Sections of 5-μm thickness were obtained by coronal cuts in microtome and then put on microscopy slides.

For gross histopathology analyses, tissue sections were stained with hematoxylin and eosin (HE); for immunohistochemistry analyses, sections of the same brain tissue were mounted on 3-aminopropyltriethoxysilane-coated (Sigma®) microscopy slides. The immunohistochemistry protocol performed in this paper was previously described by Lima et al. [23,24] and was adapted in this study. Briefly, sections were dewaxed in xylene, hydrated in decreasing ethanol solutions (absolute 2, absolute 1, 90%, 80%, and 70%), and rinsed in 0.1 M PBS for 5 min. Antigen recovery was performed with citrate buffer solution (pH 6.0), previously heated to 60 °C, for 20 min. After that, sections were further allowed to cool for 20 min and incubated in 1% hydrogen peroxide solution (H_2O_2) in methanol for 20 min to inhibition of endogenous peroxidase activity. Then, sections were rinsed three times in 0.1 M PBS/Tween (Sigma®) solution for 5 min and incubated with 10% normal goat or horse serums, for anti-GFAP and anti-NeuN, respectively, and 3% bovine serum albumin (BSA) in PBS for 2 h. Without further rinsing, sections were then incubated overnight with the primary antibody in PBS—anti-NeuN (1:100, Chemicon®) and anti-GFAP (1:2000, DAKO®)—after being rinsed in PBS/Tween solution for 5 min (three times) and incubated with biotinylated goat anti-rabbit (1:200; in GFAP sections) or horse anti-mouse (1:100; in NeuN sections) secondary antibodies (Vector Laboratories®) for 2 h. Sections were rinsed again for 5 min (three times) and incubated in the avidin-biotin-peroxidase complex (ABC Kit, Vector Laboratories®) for 2 h. Sections were rinsed three times (5 min each) in 0.1 M PBS and revealed with 3,3′ diaminobenzidine (DAB). After DAB reaction, sections were rinsed two times in 0.1 M PBS, dehydrated using alcohols and xylene, and coverslipped with Entellan (Merck®). Sections immunolabeled with anti-GFAP were counterstained with Mayer's hematoxylin.

The number of $NeuN^+$ cells and $GFAP^+$ cells was counted using a square 0.25 mm-wide grid in the eyepiece of the microscope for quantitative assessments. This grid corresponds to an area of 0.0625 mm^2. At least three fields in the motor cortex per section and three sections per animal of each group were analyzed according to the methodology described and validated by Teixeira et al. [20,25].

2.6. Statistical analyses

Data were expressed as mean ± standard error for all groups. The normality of the data was verified by the Shapiro–Wilk test. The open field test, THg accumulation, oxidative stress parameters, and immunohistochemical analyses results, were statistically analyzed by Student's t-test. The body weight gain statistical analysis was performed using one-way analysis of variance (ANOVA) with Tukey's post-hoc test. The proportional comparison of the cellular density decrease between neurons and astrocytes was tested by Fisher´s exact test. The comparison in the rotarod test was assessed by repeated measure one-way ANOVA with Holm–Sidak post-hoc test. Statistical significance was set at $p < 0.05$. All statistical analyses were performed using the GraphPad Prism 7.0 software (San Diego, California, USA).

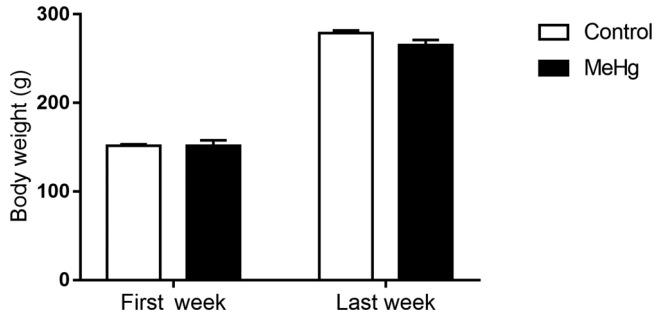

Fig. 2. Effects of MeHg (0.04 mg/kg/day) exposure during 60 days on body weight (g) of Wistar rats. The results are expressed as mean ± standard error of the mean (SEM).

3. Results

3.1. MeHg chronic low-dose exposure did not impair the body mass gain and increased the Hg levels in motor cortex neural parenchyma of rats

After the daily exposure to 40 µg/kg/day of MeHg for 60 days, all animals had gained weight ($p < 0.05$), and the animals exposed did not show differences in body mass gain by the end of the period in comparison to the control group ($p > 0.05$, Fig. 2). We also observed that even at low doses, the MeHg exposure is able to increase the THg levels in neural parenchyma of the rats' motor cortex in exposed animals (MeHg: 0.065 ± 0.019 µg/g; control: 0.004 ± 0.0007 µg/g; $p = 0.0034$; Fig. 3).

3.2. The low and chronic MeHg exposure promoted misbalance on oxidative biochemistry by increasing the pro-oxidant parameters and reducing the antioxidant defense

MeHg exposure is capable of modulating the oxidative biochemistry by reducing the ACAP levels on the motor cortex of exposed animals in about 54.05 ± 9.30%, showing a statistical difference when compared to the control group (100.00 ± 16.57%) ($p = 0.015$), as presented in Fig. 4a. Furthermore, the pro-oxidant factors were found statistically increased. The MDA levels (Fig. 4b) found in the motor cortex of animals exposed to MeHg were more than twice of those found in control ones ($p = 0.008$), while the concentration of nitrite was 94.4 ± 32.32% (Fig. 4c) higher than those of the control group ($p = 0.02$).

3.3. Chronic MeHg exposure induces histopathological changes in rat motor cortex and decreases the density of NeuN+ and GFAP+ cells

To analyze whether MeHg exposure is able to induce changes in motor cortex tissue morphology, we performed HE staining (Fig. 5). We showed that MeHg chronic exposure apparently reduced the cell density, which motivated us to evaluate and quantify the cellular density of neuron and astrocyte populations.

The comparative analysis between the studied groups showed a

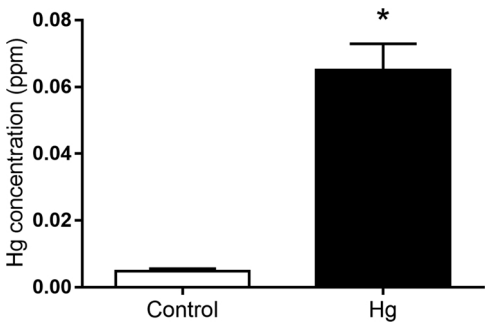

Fig. 3. Graphical representation of THg levels found in the motor cortex of adult *Wistar* rats after 60 days exposure to 40 µg/kg/day MeHg. The results are expressed as mean ± standard error of the mean (SEM). *$p < 0.05$ compared to control group (Student's t-test).

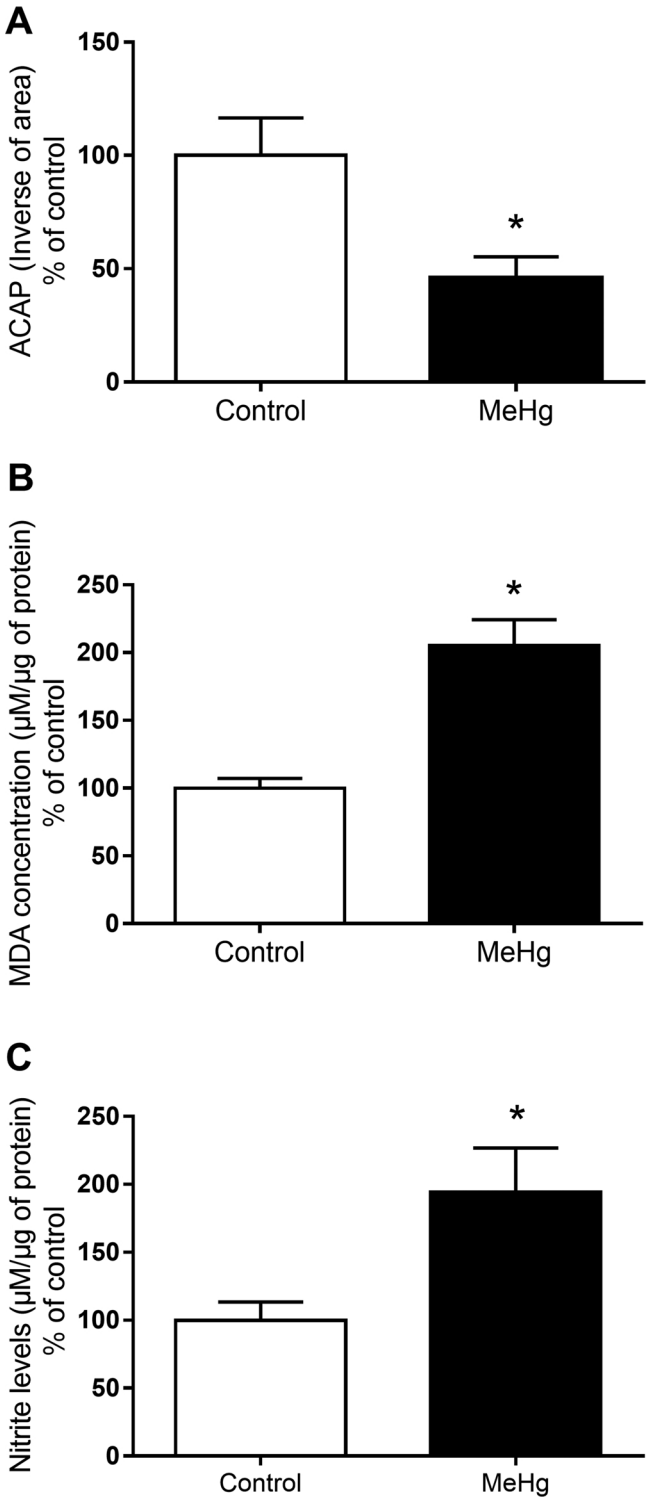

Fig. 4. Effects of chronic MeHg exposure (40 µg/kg/day), during 60 days on the motor cortex oxidative biochemistry of adults *Wistar* rats. Total antioxidant capacity against peroxyl radicals in (A), lipid peroxidation by malondialdehyde (MDA) levels (B) and nitrite levels (C). The results are expressed as mean ± standard error of the mean (SEM) ($n = 10$ animals per group). *$p < 0.05$ compared to control group (Student's t-test).

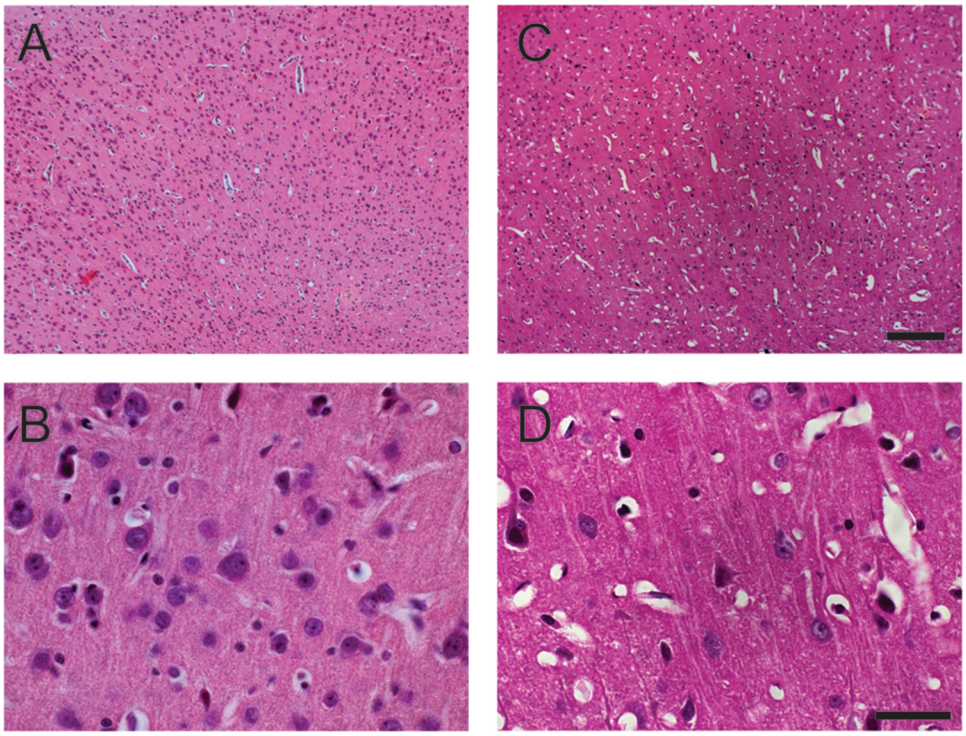

Fig. 5. Effects of chronic MeHg exposure (40 µg/kg/day), during 60 days on the morphology of the motor cortex of adult *Wistar* rats. Sections were stained with hematoxylin and eosin (HE). Control animals administered corn oil (A and B) and exposed animals MeHg (C and D). Scale bars: 100 µm (A and C); 30 µm (B and D).

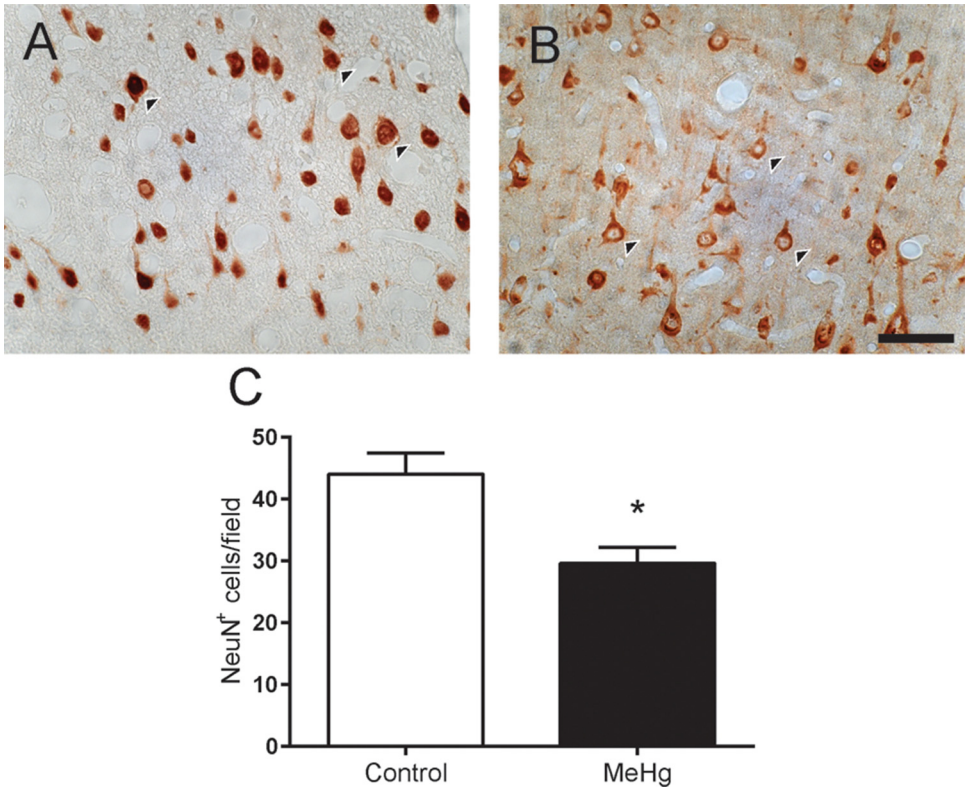

Fig. 6. Effects of chronic MeHg exposure (40 µg/kg/day), during 60 days on $NeuN^+$ cells in the motor cortex of adults *Wistar* rats. Arrowhead indicates $NeuN^+$ cells. Panel A showing photomicrographs $NeuN^+$ cells in the control group and the panel B represents MeHg-exposed group. Panel C represents $NeuN^+$ cells density (n = 10 animals per group). The results are expressed as mean ± standard error of the mean (SEM). *p < 0.05 compared to control group (Student's t-test). Scale bars: 30 µm.

reduction in the NeuN+ cell population of MeHg-exposed animals (29.64 ± 2.60) compared to the control group (44.07 ± 3.40; p = 0.007; Fig.6). In addition, the number of GFAP+ cells in the Hg-exposed group was also reduced (MeHg: 17.79 ± 1.20; control: 37.94 ± 1.22; p = 0.007; Fig. 7). Interestingly, the decrease in the neuronal population (67.25%) was significantly higher than that observed in the astrocytic population (46.89%) (Fisher´s exact test, p < 0.05)

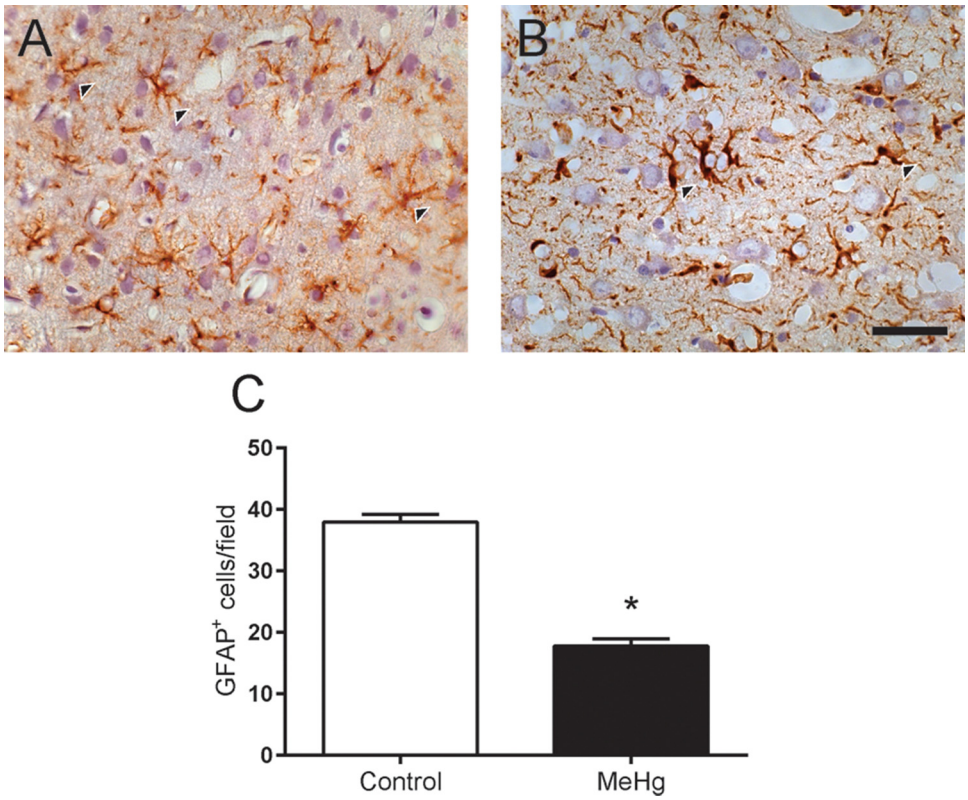

Fig. 7. Effects of chronic MeHg exposure (40 µg/kg/day), during 60 days on GFAP$^+$ cells in the motor cortex of adult *Wistar* rats. Arrowhead indicates GFAP$^+$ cells. Board A represents photomicrographs showing GFAP$^+$ cells in the control group and the board B showing MeHg-exposed group. Board C re-present GFAP$^+$ cells density (n = 10 animals per group). The results are expressed as mean ± standard error of the mean (SEM). *p < 0.05 compared to control group (Student's t-test). Scale bar: 30 µm.

3.4. Biochemical and morphological alterations in the motor cortex were reflected in poor performance of motor function assays

The spontaneous locomotor activity performed by the animals is represented on the tracking plot (Fig. 8a), showing a representative plot of exploratory activity performed by the animals. The peripheral distance executed by exposed animals was lower than in the control group (MeHg: 7.93 ± 1.34; control: 13.72 ± 0.84; p = 0.0019; Fig. 8b). No difference was observed in the central distance performed between the two groups (p = 0.8774; Fig. 8b), reinforcing that the motor

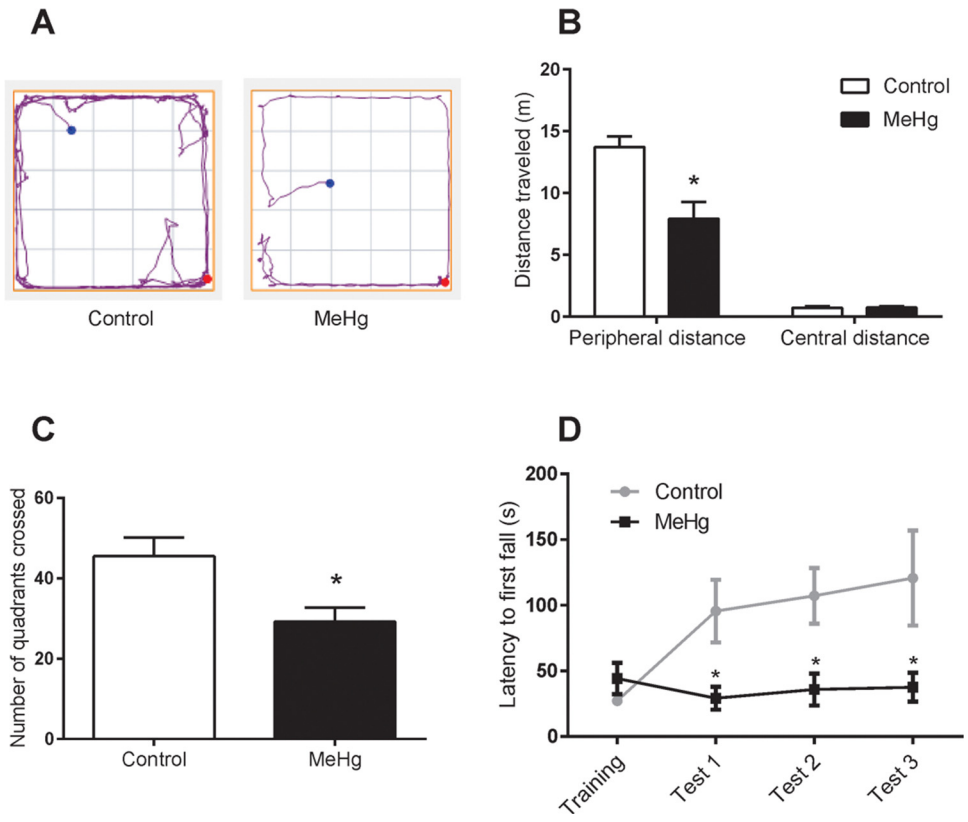

Fig. 8. Behavioral evaluation of adult *Wistar* rats chronically exposed to low doses of MeHg (40 µg/Kg) (n = 10 animals per group). Tracking Plot (A), distance traveled in the center and periphery (B), number of total quadrants crossed (C) and latency of first fall (E). The results are expressed as mean ± standard error of the mean (SEM). Open field test (A–C): *p < 0.05 compared to control group. Rotarod test (D): *p < 0.05 (repeated measure one-way ANOVA with Holm–Sidak post-hoc test).

impairment was not related to an anxiety-like behavior, once the central distance performed did not show differences in comparison to the control group.

Furthermore, the MeHg group had a lower number of total quadrants crossed (MeHg: 29.22 ± 3.52; control: 45.50 ± 4.69; $p = 0.01$; Fig. 8c) in comparison to the control group. In the forced coordinating test (rotarod), repeated measure ANOVA showed that MeHg intoxication elicited lower latency to the first fall in all test sessions after training (Fig. 8d), suggesting motor coordination impairment (interaction: $p < 0.0210$; treatment: $p < 0.0001$).

4. Discussion

In our study, chronic MeHg exposure in adult rats, which simulates lifelong human MeHg exposure, resulted in Hg accumulation in the motor cortex, oxidative stress, and a reduced number of neurons and astrocytes, which consequently generated alterations of motor skills.

This model is representative of the chronic exposure of fish-eating populations around the world, such as those found in the Amazon [3,9]. Deleterious consequences such as genotoxic, pro-oxidant, and, mainly, neurofunctional alterations have already been described in Amazonian populations [26–29]. The minimum levels of THg found in these populations is about 2–3 μg/g in hair, which is equivalent to approximately 0.06 μg/g in the brain, according to the proportion 250:5:1 for hair:brain:blood in humans [8]. The latter level of Hg (0.06 μg/g in the brain) is similar to that observed in the cortex of exposed animals (Fig. 3), confirming the importance of the present model to elucidate brain alterations caused by an exposure relevant for human populations.

The motor cortex, the anatomical area chosen for our investigation, is considered the main source of voluntary cortical motor commands [30], receiving afferents from the prefrontal cortex and parietal cortex, projecting them to the thalamus, cerebellum, and spinal cord [31,32]. Although neural control of motion begins in the prefrontal cortex and is modulated by the basal and cerebellar ganglia, the motor cortex is the main effector area for descending pathways [30].

In this way, considering the role played by the motor cortex, this region is the subject of study in several investigations that evaluate its alterations in animal models facing exposure to metals [5,7,33,34]. The CNS is reported as an important target of MeHg action, characterizing a region of tropism, and the mechanisms of toxicity in MeHg exposure models are widely debated (for review, see Farina [35]). Among them, the imbalance between oxidative and reductive cellular processes is critical for MeHg-induced neurotoxicity [36].

Regarding this problem, the MeHg neurotoxicity potential through the increase of reactive oxygen and nitrogen species (RONS) generation is well established in a number of experimental models [37–40]. In the present study, nitrite levels were elevated in the motor cortex of exposed rats, indicating an increased production of nitrites due to MeHg exposure. Associated to this effect, the antioxidant capacity was decreased and LPO increased in the adult rats chronically exposed to this organometallic compound. These findings are probably related to the high affinity of MeHg to sulfhydryl (thiol) groups (-SH). Several *in vivo* and *in vitro* studies have shown that MeHg covalently binds to –SH groups of enzymatic and non-enzymatic molecules, thereby inactivating them [41–46]. The major intracellular antioxidant in all tissues, due to its abundance (1–10 mM), is glutathione (GSH), a low-molecular-weight thiol compound [47]. The Hg atom in MeHg binds with the thiol group of GSH, leading to the formation of the complex GS-$HgCH_3$ [48]. This complex is excreted from the cell, lowering the GSH intracellular concentration and thus depleting the antioxidant competence of the tissue [49], which, in turn, leads to an excess of non-intercepted prooxidants and oxidative damage, showed in the present study as an increase in nitrite concentration and LPO, respectively

Huang et al. [50,51] exposed mice to a low dose of MeHg (50 and 20 μg/kg/day, respectively) for seven weeks and analyzed brain tissues (cerebral and cerebellar cortex) and blood. In both studies, chronic MeHg exposure resulted in alteration of LPO, Na^+, K^+-ATPase activity, and nitric oxide (NO) in the same brain tissues and blood. It is important to point out that there are other important routes of MeHg oxidative stress-induced neurotoxicity that are probably acting together with the described mechanism. These pathways include the inactivation and thus dysfunction of important thiol enzymes (tyrosine phosphatase and creatine kinase) and selenoproteins (thioredoxins and thioredoxin reductase) [35].

In addition, according to our oxidative biochemistry analyses, the motor cortex showed to be susceptible to Hg damage, decreasing antioxidant capacity, and increasing LPO and nitrite levels. Modulation of oxidative stress parameters has already been demonstrated in other brain regions like the cerebellum, hypothalamus, and cerebral cortex, as well as in the total brain [50,52–55].

Furthermore, RONS are also related to a drive to oxidative DNA resulting in cell death or tissue injury within the central and peripheral nervous system [51,56]. In this case, the oxidative stress caused by MeHg exposure probably acts on the classic pathways of apoptosis initiation through a mitochondrial oxidative chain [57] associated with an increase of intracellular Ca^{2+} (described below; Chan [58]) or even by activating multiple cell death pathways concomitantly [59]. Thus, one of the hypotheses of MeHg toxicity is based on mitochondrial respiratory chain breakdown, resulting in increased peroxide levels in the motor cortex and, consequently, disruption of the cell proliferation process and cell death by apoptosis [60]. However, it is clear that MeHg neurotoxicity depends on cell type [59].

Astrocytes were previously reported as a preferential site of MeHg accumulation [61–64]. Additionally, significant reductions in the number of neurons were also observed and previously described in other studies that analyzed CNS and MeHg exposure [35,65,66]. Interestingly, exposure to the same concentration of MeHg caused greater accumulation of this organometal in glial-origin cells than in cells of neuronal origin [67], but lower cell death [68]. This preferential accumulation in glial cells may protect neurons by removing the metal from the extracellular environment. The high susceptibility of neurons to MeHg exposure was demonstrated *in vivo* in our work with a 67.25% decrease in number of neurons and 46.89% decrease in number of glial cells (Fig. 6 and 7).

In this way, astrocytes have been described as the preferential site of accumulation of MeHg [69]. They play an essential role in the development, function, and plasticity of the brain. These cells coordinate neuronal development and survival, control the formation and function of synapses, and play an important role in the formation of neuronal circuits [34,70,71]. In addition, astrocytes perform other critical functions in the brain, including the formation of the blood–brain barrier and the expression of neurotransmitter transporters [72]. Damage in astrocyte cells caused by exposure to MeHg generates imbalance in the perineuronal parenchymal homeostasis. This imbalance leads to increased permeability of the blood–brain barrier, oxidative damage, and cytoskeletal disruption [35,61,73–75].

These findings are in line with previous reports showing that MeHg disrupted the homeostasis of the phosphorylation system associated with the cytoskeletal proteins of astrocytes and neurons in the motor cortex [41,76]. However, neurons seem to be more susceptible to the toxic effects of MeHg, probably due to the loss of protection by astrocytes against MeHg, or neuronal death by apoptosis may be the end point of the neurotoxicity of MeHg [77,78].

Additionally, neuronal death is directly linked to the decrease in astrocyte number. The main mechanism of neuronal protection played by glia consists in reducing the bioavailability of excessive glutamate in the synaptic cleft in order to avoid excitotoxicity [79]. In this way, Aschner et al. [63] exhaustively described how MeHg plays an important role in excitotoxicity, once this event propitiates the parallel intracellular calcium overload, which is related to increased Ca^{2+} in the mitochondrial matrix and its further dysfunction, with consecutive

opening of pores in the mitochondrial membrane and release of cytochrome c and apoptotic factors, such as caspases and pro-caspases [36,80]. In this way, we believe that neuronal death is a second result of glial failure, once the neuronal microenvironment is misbalanced. In this sense, considering the importance of pyramidal neurons in cell communication in the motor cortex for motor performance, MeHg exposure damaged this structure, possibly leading to the poor motor skills observed in this study.

Although other areas of the CNS also participate in motor function as cited above, the motor cortex plays an essential function in fine motor control and fractionation of movement sensorimotor integration, besides acting in higher-order cognitive–motor movements [20,81]. Actually, our low MeHg intoxication paradigm with loss of brain cells in the motor cortex (*e.g.* neurons and astrocytes) reflected in poor motor performance. Motor function was assessed by two ethological and different paradigms. The first one is related to purposive motor behavior (*e.g.* open field) in an area that has been directly related to cortical areas [82]. On the other hand, the second paradigm (rotarod test) is sensible to demonstrate gross motor deficits, in which the fear of fall is considered the motivational stimulus to maintain itself on the rotating rod. This also reflects motor learning through successive exposures of individuals (for review, see Brooks and Dunnett [83]).

Our data support the evidence that the neurodegeneration observed in the motor cortical area was reflected in ethological behavior alteration, with a reduced spontaneous exploration profile. Indeed, to add a stimulus to perform a motor task, such as fear, we employed the rotarod paradigm. In this assay, the motor cortex degeneration induced by MeHg exposure reduced the latency to first fall, even after successive exposures.

5. Conclusion

In conclusion, we showed that MeHg exposure during adulthood in rats, at similar doses to which humans are exposed in contaminated environments, is capable of triggering oxidative stress and neurodegeneration in the motor cortex, promoting impairments to the primordial motor functions.

Conflict of interest

The authors d eclare there is no conflict of interest

Acknowledgments

This work was supported by the Brazilian National Council for Scientific and Technological Development (CNPq), Fundação de Amparo a Pesquisa do Estado do Pará (FAPESPA), and Pró-Reitoria de Pesquisa e Pós-Graduação da UFPA (PROPESP, UFPA, Brazil).

References

[1] T.W. Clarkson, L. Magos, The toxicology of mercury and its chemical compounds, Crit. Rev. Toxicol. 36 (8) (2006) 609–662.
[2] M.C. Bisinoti, W.F. Jardim, O comportamento do metilmercúrio (metilHg) no ambiente, Química Nova 27 (2004) 593–600.
[3] G.P.F. Arrifano, R.C.R. Martin-Doimeadios, M. Jimenez-Moreno, V. Ramirez-Mateos, N.F.S. da Silva, J.R. Souza-Monteiro, M. Augusto-Oliveira, R.S.O. Paraense, B.M. Macchi, J.L.M. do Nascimento, M.E. Crespo-Lopez, Large-scale projects in the amazon and human exposure to mercury: the case-study of the Tucurui Dam, Ecotoxicol. Environ. Saf. 147 (2018) 299–305.
[4] R.C. Rodriguez Martin-Doimeadios, J.J. Berzas Nevado, F.J. Guzman Bernardo, M. Jimenez Moreno, G.P. Arrifano, A.M. Herculano, J.L. do Nascimento, M.E. Crespo-Lopez, Comparative study of mercury speciation in commercial fishes of the Brazilian Amazon, Environ. Sci. Pollut. Res. Int. 21 (12) (2014) 7466–7479.
[5] M. Farina, M. Aschner, Methylmercury-induced neurotoxicity: focus on pro-oxidative events and related consequences, Adv. Neurobiol. 18 (2017) 267–286.
[6] R.A. Bernhoft, Mercury toxicity and treatment: a review of the literature, J. Environ. Public. Health (2012) (2012) 460508.
[7] H.K. Kong, M.H. Wong, H.M. Chan, S.C. Lo, Chronic exposure of adult rats to low doses of methylmercury induced a state of metabolic deficit in the somatosensory cortex, J. Proteome Res. 12 (11) (2013) 5233–5245.
[8] V. Branco, S. Caito, M. Farina, J. Teixeira da Rocha, M. Aschner, C. Carvalho, Biomarkers of mercury toxicity: past, present, and future trends, J. Toxicol. Environ. Health B Crit. Rev. 20 (3) (2017) 119–154.
[9] J.J. Berzas Nevado, R.C. Rodriguez Martin-Doimeadios, F.J. Guzman Bernardo, M. Jimenez Moreno, A.M. Herculano, J.L. do Nascimento, M.E. Crespo-Lopez, Mercury in the Tapajos River basin, Brazilian Amazon: a review, Environ. Int. 36 (6) (2010) 593–608.
[10] Q. Wu, W.K. Li, Z.P. Zhou, Y.Y. Li, T.W. Xiong, Y.Z. Du, L.X. Wei, J. Liu, The Tibetan medicine Zuotai differs from HgCl2 and MeHg in producing liver injury in mice, Regul. Toxicol. Pharmacol.: RTP 78 (2016) 1–7.
[11] M. Rafati-Rahimzadeh, M. Rafati-Rahimzadeh, S. Kazemi, A.A. Moghadamnia, Current approaches of the management of mercury poisoning: need of the hour, DARU J. Pharm. Sci. 22 (1) (2014) 46-46.
[12] L.O. Bittencourt, B. Puty, S. Charone, W.A.B. Arago, P.M. Farias-Junior, M.C.F. Silva, M.E. Crespo-Lopez, Ad.L. Leite, M.A.R. Buzalaf, R.R. Lima, Oxidative biochemistry disbalance and changes on proteomic profile in salivary glands of rats induced by chronic exposure to methylmercury, Oxid. Med. Cell. Longev. (2017) (2017) 15.
[13] L.A.O. Lima, L.O. Bittencourt, B. Puty, R.M. Fernandes, P.C. Nascimento, M.C.F. Silva, S.M. Alves-Junior, J.J.V. Pinheiro, R.R. Lima, Methylmercury intoxication promotes metallothionein response and cell damage in salivary glands of rats, Biol. Trace Elem. Res. (2018).
[14] R.N. Walsh, R.A. Cummins, The open-field test: a critical review, Psychol. Bull. 83 (3) (1976) 482–504.
[15] N.W. Dunham, T.S. Miya, A note on a simple apparatus for detecting neurological deficit in rats and mice, J. Am. Pharm. Assoc. 46 (3) (1957) 208–209.
[16] F.B. Teixeira, R.M. Fernandes, P.M. Farias-Junior, N.M. Costa, L.M. Fernandes, L.N. Santana, A.F. Silva-Junior, M.C. Silva, C.S. Maia, R.R. Lima, Evaluation of the effects of chronic intoxication with inorganic mercury on memory and motor control in rats, Int. J. Environ. Res. Public Health 11 (9) (2014) 9171–9185.
[17] H. Akagi, H. Nishimura, Speciation of mercury in the environment, in: T. Suzuki, N. Imura, T.W. Clarkson (Eds.), Advances in Mercury Toxicology, Springer, US, Boston, MA, 1991, pp. 53–76.
[18] L.L. Amado, M.L. Garcia, P.B. Ramos, R.F. Freitas, B. Zafalon, J.L. Ferreira, J.S. Yunes, J.M. Monserrat, A method to measure total antioxidant capacity against peroxyl radicals in aquatic organisms: application to evaluate microcystins toxicity, Sci. Total Environ. 407 (6) (2009) 2115–2123.
[19] L.C. Green, D.A. Wagner, J. Glogowski, P.L. Skipper, J.S. Wishnok, S.R. Tannenbaum, Analysis of nitrate, nitrite, and [15N]nitrate in biological fluids, Anal. Biochem. 126 (1) (1982) 131–138.
[20] F.B. Teixeira, L.N. Santana, F.R. Bezerra, S. De Carvalho, E.A. Fontes-Junior, R.D. Prediger, M.E. Crespo-Lopez, C.S. Maia, R.R. Lima, Chronic ethanol exposure during adolescence in rats induces motor impairments and cerebral cortex damage associated with oxidative stress, PloS One 9 (6) (2014) e101074.
[21] J.R. Souza-Monteiro, M. Hamoy, D. Santana-Coelho, G.P. Arrifano, R.S. Paraense, A. Costa-Malaquias, J.R. Mendonca, R.F. da Silva, W.S. Monteiro, H. Rogez, D.L. de Oliveira, J.L. do Nascimento, M.E. Crespo-Lopez, Anticonvulsant properties of Euterpe oleracea in mice, Neurochem. Int. 90 (2015) 20–27.
[22] M.M. Bradford, A rapid and sensitive method for the quantitation of microgram quantities of protein utilizing the principle of protein-dye binding, Anal. Biochem. 72 (1) (1976) 248–254.
[23] R.R. Lima, J. Guimaraes-Silva, J.L. Oliveira, A.M. Costa, R.D. Souza-Rodrigues, C.D. Dos Santos, C.W. Picanco-Diniz, W. Gomes-Leal, Diffuse axonal damage, myelin impairment, astrocytosis and inflammatory response following microinjections of NMDA into the rat striatum, Inflammation 31 (1) (2008) 24–35.
[24] Rafael R. Lima, Luana N.S. Santana, Rafael M. Fernandes, Elder M. Nascimento, Ana Carolina A. Oliveira, Luanna M.P. Ferna, Neurodegeneration and glial response after acute striatal stroke: histological basis for neuroprotective studies, Oxid. Med. Cell. Longev. (2016) (2016) 15.
[25] F.B. Teixeira, A.C.A. de Oliveira, L.K.R. Leão, N.C.F. Fagundes, R.M. Fernandes, L.M.P. Fernandes, M.C.F. da Silva, L.L. Amado, F.E.S. Sagica, E.H.C. de Oliveira, M.E. Crespo-Lopez, C.S.F. Maia, R.R. Lima, Exposure to inorganic mercury causes oxidative stress, cell death, and functional deficits in the motor cortex, Front. Mol. Neurosci. 11 (125) (2018).
[26] M.E. Crespo-Lopez, G.L. Macedo, G.P. Arrifano, C. Pinheiro Mda, J.L. do Nascimento, A.M. Herculano, Genotoxicity of mercury: contributing for the analysis of Amazonian populations, Environ. Int. 37 (1) (2011) 136–141.
[27] J. Dolbec, D. Mergler, C.J. Sousa Passos, S. Sousa de Morais, J. Lebel, Methylmercury exposure affects motor performance of a riverine population of the Tapajos river, Brazilian Amazon, Int. Arch. Occup. Environ. Health 73 (3) (2000) 195–203.
[28] M. Fillion, A. Philibert, F. Mertens, M. Lemire, C.J. Passos, B. Frenette, J.R. Guimaraes, D. Mergler, Neurotoxic sequelae of mercury exposure: an intervention and follow-up study in the Brazilian Amazon, EcoHealth 8 (2) (2011) 210–222.
[29] M.C. Pinheiro, B.M. Macchi, J.L. Vieira, T. Oikawa, W.W. Amoras, G.A. Guimaraes, C.A. Costa, M.E. Crespo-Lopez, A.M. Herculano, L.C. Silveira, J.L. do Nascimento, mercury exposure and antioxidant defenses in women: a comparative study in the amazon, Environ. Res. 107 (1) (2008) 53–59.
[30] R.N. Lemon, Descending pathways in motor control, Annu. Rev. Neurosci. 31 (2008) 195–218.
[31] B. Pollok, K. Stephan, A. Keitel, V. Krause, N.K. Schaal, The posterior parietal cortex subserves precise motor timing in professional drummers, Front. Hum. Neurosci. 11 (183) (2017).
[32] P.L. Sheets, G.M. Shepherd, Cortical circuits for motor control,

Neuropsychopharmacol. 36 (1) (2011) 365–366.
[33] R. Pamphlett, S. Kum Jew, Heavy metals in locus ceruleus and motor neurons in motor neuron disease, Acta Neuropathol. Commun. 1 (2013) 81.
[34] C. Eskes, P. Honegger, L. Juillerat-Jeanneret, F. Monnet-Tschudi, Microglial reaction induced by noncytotoxic methylmercury treatment leads to neuroprotection via interactions with astrocytes and IL-6 release, Glia 37 (1) (2002) 43–52.
[35] M. Farina, J.B. Rocha, M. Aschner, Mechanisms of methylmercury-induced neurotoxicity: evidence from experimental studies, Life Sci. 89 (15-16) (2011) 555–563.
[36] J.L. do Nascimento, K.R. Oliveira, M.E. Crespo-Lopez, B.M. Macchi, L.A. Maues, C. Pinheiro Mda, L.C. Silveira, A.M. Herculano, Methylmercury neurotoxicity & antioxidant defenses, Indian J. Med. Res. 128 (4) (2008) 373–382.
[37] S.F. Ali, C.P. LeBel, S.C. Bondy, Reactive oxygen species formation as a biomarker of methylmercury and trimethyltin neurotoxicity, Neurotoxicology 13 (3) (1992) 637–648.
[38] S.T. Park, K.T. Lim, Y.T. Chung, S.U. Kim, Methylmercury-induced neurotoxicity in cerebral neuron culture is blocked by antioxidants and NMDA receptor antagonists, Neurotoxicology 17 (1) (1996) 37–45.
[39] T.A. Sarafian, L. Vartavarian, D.J. Kane, D.E. Bredesen, M.A. Verity, Bcl-2 expression decreases methyl mercury-induced free-radical generation and cell killing in a neural cell line, Toxicol. Lett. 74 (2) (1994) 149–155.
[40] O. Sorg, B. Schilter, P. Honegger, F. Monnet-Tschudi, Increased vulnerability of neurones and glial cells to low concentrations of methylmercury in a prooxidant situation, Acta Neuropathol. 96 (6) (1998) 621–627.
[41] M. Aschner, T. Syversen, Methylmercury: recent advances in the understanding of its neurotoxicity, Ther. Drug Monit. 27 (3) (2005) 278–283.
[42] F.L. Hastings, G.W. Lucier, R. Klein, Methylmercury-cholinesterase interactions in rats, Environ. Health Perspect. 12 (1975) 127–130.
[43] K. Kageyama, Y. Onoyama, E. Kano, Effects of methyl mercuric chloride and sulfhydryl inhibitors on phospholipid synthetic activity of lymphocytes, J. Appl. Toxicol.: JAT 6 (1) (1986) 49–53.
[44] F. Kanda, T. Kamikashi, S. Ishibashi, Competitive inhibition of hexokinase isoenzymes by mercurials, J. Biochem. 79 (3) (1976) 543–548.
[45] M.P. Kung, P. Kostyniak, J. Olson, M. Malone, J.A. Roth, Studies of the in vitro effect of methylmercury chloride on rat brain neurotransmitter enzymes, J. Appl. Toxicol.: JAT 7 (2) (1987) 119–121.
[46] S. Magour, Studies on the inhibition of brain synaptosomal Na+/K+-ATPase by mercury chloride and methyl mercury chloride, Arch. Toxicol. Suppl. = Archiv fur Toxikologie. Suppl. 9 (1986) 393–396.
[47] A.J. Cooper, B.S. Kristal, Multiple roles of glutathione in the central nervous system, Biol. Chem. 378 (8) (1997) 793–802.
[48] N. Ballatori, T.W. Clarkson, Developmental changes in the biliary excretion of methylmercury and glutathione, Sci. (New York, N.Y.) 216 (4541) (1982) 61–63.
[49] N. Ballatori, S.M. Krance, S. Notenboom, S. Shi, K. Tieu, C.L. Hammond, Glutathione dysregulation and the etiology and progression of human diseases, Biol. Chem. 390 (3) (2009) 191–214.
[50] C.F. Huang, C.J. Hsu, S.H. Liu, S.Y. Lin-Shiau, Neurotoxicological mechanism of methylmercury induced by low-dose and long-term exposure in mice: oxidative stress and down-regulated Na+/K(+)-ATPase involved, Toxicol. Lett. 176 (3) (2008) 188–197.
[51] C.F. Huang, S.H. Liu, C.J. Hsu, S.Y. Lin-Shiau, Neurotoxicological effects of low-dose methylmercury and mercuric chloride in developing offspring mice, Toxicol. Lett. 201 (3) (2011) 196–204.
[52] H.R. Andersen, O. Andersen, Effects of dietary alpha-tocopherol and beta-carotene on lipid peroxidation induced by methyl mercuric chloride in mice, Pharmacol. Toxicol. 73 (4) (1993) 192–201.
[53] P. Kaur, M. Aschner, T. Syversen, Biochemical factors modulating cellular neurotoxicity of methylmercury, J. Toxicol. (2011) (2011) 9.
[54] D.F. Meinerz, M.T. de Paula, B. Comparsi, M.U. Silva, A.E. Schmitz, H.C. Braga, P.S. Taube, A.L. Braga, J.B. Rocha, A.L. Dafre, M. Farina, J.L. Franco, T. Posser, Protective effects of organoselenium compounds against methylmercury-induced oxidative stress in mouse brain mitochondrial-enriched fractions, Braz. J. Med. Biol. Res. = Revista brasileira de pesquisas medicas e biologicas 44 (11) (2011) 1156–1163.
[55] W. Liu, Z. Xu, Y. Deng, B. Xu, Y. Wei, T. Yang, Protective effects of memantine against methylmercury-induced glutamate dyshomeostasis and oxidative stress in rat cerebral cortex, Neurotoxic. Res. 24 (3) (2013) 320–337.
[56] M.E. Crespo-Lopez, G.L. Macedo, S.I. Pereira, G.P. Arrifano, D.L. Picanco-Diniz, J.L. do Nascimento, A.M. Herculano, Mercury and human genotoxicity: critical considerations and possible molecular mechanisms, Pharmacol. Res. 60 (4) (2009) 212–220.
[57] P. Kaur, M. Aschner, T. Syversen, Glutathione modulation influences methyl mercury induced neurotoxicity in primary cell cultures of neurons and astrocytes, Neurotoxicology 27 (4) (2006) 492–500.
[58] S.L. Chan, M.P. Mattson, Caspase and calpain substrates: roles in synaptic plasticity and cell death, J. Neurosci. Res. 58 (1) (1999) 167–190.
[59] S. Ceccatelli, E. Dare, M. Moors, Methylmercury-induced neurotoxicity and apoptosis, Chem. Biol. Interact. 188 (2) (2010) 301–308.
[60] V. Sava, O. Reunova, A. Velasquez, S. Song, J. Sanchez-Ramos, Neuroanatomical mapping of DNA repair and antioxidative responses in mouse brain: effects of a single dose of MPTP, Neurotoxicology 27 (6) (2006) 1080–1093.
[61] J.W. Allen, L.A. Mutkus, M. Aschner, Mercuric chloride, but not methylmercury, inhibits glutamine synthetase activity in primary cultures of cortical astrocytes, Brain Res. 891 (1-2) (2001) 148–157.
[62] M. Aschner, Astrocytes as modulators of mercury-induced neurotoxicity, Neurotoxicology 17 (3-4) (1996) 663–669.
[63] M. Aschner, C.P. Yao, J.W. Allen, K.H. Tan, Methylmercury alters glutamate transport in astrocytes, Neurochem. Int. 37 (2-3) (2000) 199–206.
[64] J.S. Charleston, R.L. Body, R.P. Bolender, N.K. Mottet, M.E. Vahter, T.M. Burbacher, Changes in the number of astrocytes and microglia in the thalamus of the monkey Macaca fascicularis following long-term subclinical methylmercury exposure, Neurotoxicology 17 (1) (1996) 127–138.
[65] C.M. Carvalho, E.H. Chew, S.I. Hashemy, J. Lu, A. Holmgren, Inhibition of the human thioredoxin system. A molecular mechanism of mercury toxicity, J. Biol. Chem. 283 (18) (2008) 11913–11923.
[66] A. Falluel-Morel, K. Sokolowski, H.M. Sisti, X. Zhou, T.J. Shors, E. Dicicco-Bloom, Developmental mercury exposure elicits acute hippocampal cell death, reductions in neurogenesis, and severe learning deficits during puberty, J. Neurochem. 103 (5) (2007) 1968–1981.
[67] J.J.B. Nevado, R.C.R. Martín-Doimeadios, M.J. Moreno, J.L.M. do Nascimento, A.M. Herculano, M.E. Crespo-López, Mercury speciation analysis on cell lines of the human central nervous system to explain genotoxic effects, Microchem. J. 93 (1) (2009) 12–16.
[68] M.E. Crespo-López, A. Lima de Sá, A.M. Herculano, R. Rodríguez Burbano, J.L. Martins do Nascimento, Methylmercury genotoxicity: a novel effect in human cell lines of the central nervous system, Environ. Int. 33 (2) (2007) 141–146.
[69] M.R. Carratu, P. Borracci, A. Coluccia, A. Giustino, G. Renna, M.C. Tomasini, E. Raisi, T. Antonelli, V. Cuomo, E. Mazzoni, L. Ferraro, Acute exposure to methylmercury at two developmental windows: focus on neurobehavioral and neurochemical effects in rat offspring, Neuroscience 141 (3) (2006) 1619–1629.
[70] T. Nishioku, N. Takai, K. Miyamoto, K. Murao, C. Hara, K. Yamamoto, H. Nakanishi, Involvement of caspase 3-like protease in methylmercury-induced apoptosis of primary cultured rat cerebral microglia, Brain Res. 871 (1) (2000) 160–164.
[71] J. Mitra, E.N. Guerrero, P.M. Hegde, H. Wang, I. Boldogh, K.S. Rao, S. Mitra, M.L. Hegde, New perspectives on oxidized genome damage and repair inhibition by pro-oxidant metals in neurological diseases, Biomolecules 4 (3) (2014) 678–703.
[72] Z. Yin, D. Milatovic, J.L. Aschner, T. Syversen, J.B. Rocha, D.O. Souza, M. Sidoryk, J. Albrecht, M. Aschner, Methylmercury induces oxidative injury, alterations in permeability and glutamine transport in cultured astrocytes, Brain Res. 1131 (1) (2007) 1–10.
[73] L.T. Zimmermann, D.B. dos Santos, D. Colle, A.A. dos Santos, M.A. Hort, S.C. Garcia, L.P. Bressan, D. Bohrer, M. Farina, Methionine stimulates motor impairment and cerebellar mercury deposition in methylmercury-exposed mice, J. Toxicol. Environ. Health A 77 (1-3) (2014) 46–56.
[74] C. Johansson, A.F. Castoldi, N. Onishchenko, L. Manzo, M. Vahter, S. Ceccatelli, Neurobehavioural and molecular changes induced by methylmercury exposure during development, Neurotoxic. Res. 11 (3-4) (2007) 241–260.
[75] T. Takahashi, M. Fujimura, M. Koyama, M. Kanazawa, F. Usuki, M. Nishizawa, T. Shimohata, Methylmercury causes blood-brain barrier damage in rats via upregulation of vascular endothelial growth factor expression, PloS One 12 (1) (2017) e0170623.
[76] F. Castoldi Anna, S. Barni, I. Turin, C. Gandini, L. Manzo, Early acute necrosis, delayed apoptosis and cytoskeletal breakdown in cultured cerebellar granule neurons exposed to methylmercury, J. Neurosci. Res. 59 (6) (2000) 775–787.
[77] Y. Noguchi, Y. Shinozaki, K. Fujishita, K. Shibata, Y. Imura, Y. Morizawa, C. Gachet, S. Koizumi, astrocytes protect neurons against methylmercury via ATP/P2Y1 receptor-mediated pathways in astrocytes, PloS One 8 (2) (2013) e57898.
[78] W.R. Mundy, T.M. Freudenrich, Sensitivity of immature neurons in culture to metal-induced changes in reactive oxygen species and intracellular free calcium, Neurotoxicology 21 (6) (2000) 1135–1144.
[79] Y.-B. Ouyang, L. Xu, S. Liu, R.G. Giffard, Role of astrocytes in delayed neuronal death: GLT-1 and its novel regulation by microRNAs, Adv. Neurobiol. 11 (2014) 171–188.
[80] D.W. Choi, Ischemia-induced neuronal apoptosis, Curr. Opin. Neurobiol. 6 (5) (1996) 667–672.
[81] W.W. Teka, K.C. Hamade, W.H. Barnett, T. Kim, S.N. Markin, I.A. Rybak, Y.I. Molkov, From the motor cortex to the movement and back again, PloS One 12 (6) (2017) e0179288.
[82] K.V. Shenoy, M. Sahani, M.M. Churchland, Cortical control of arm movements: a dynamical systems perspective, Annu. Rev. Neurosci. 36 (2013) 337–359.
[83] S.P. Brooks, S.B. Dunnett, Tests to assess motor phenotype in mice: a user's guide, Nat. Rev., Neurosci. 10 (7) (2009) 519–529.